

Excited state intramolecular charge transfer reaction of 4-(morpholenyl)benzonitrile in solution: Effects of hetero atom in the donor moiety

TUHIN PRADHAN, HARUN AL RASID GAZI and RANJIT BISWAS*

Department of Chemical, Biological and Macromolecular Sciences,
S.N. Bose National Centre for Basic Sciences, J.D. Block, Sector III, Salt Lake, Kolkata 700 098
e-mail: ranjit@bose.res.in

MS received 14 January 2010; revised 16 June 2010; accepted 18 June 2010

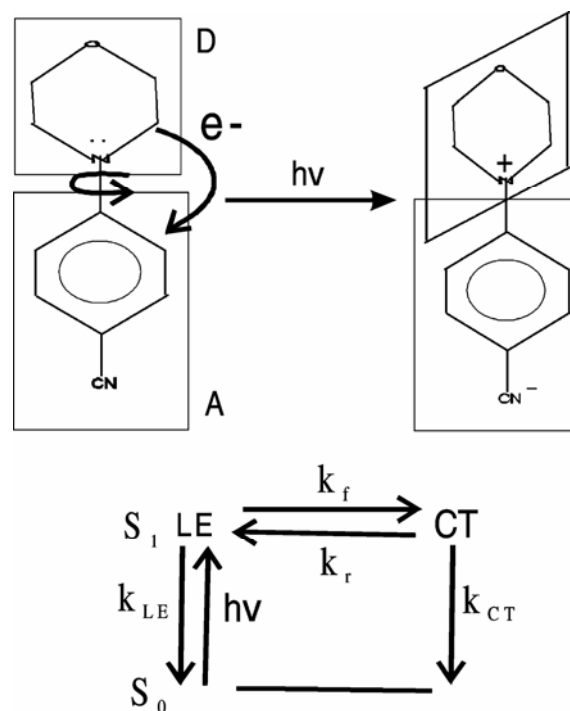
Abstract. An intramolecular charge transfer (ICT) molecule with an extra hetero atom in its donor moiety has been synthesized in order to investigate how ICT reaction is affected by hetero atom replacement. Photo-physical and photo-dynamical properties of this molecule, 4-(morpholenyl)benzonitrile (M6C), have been studied in 20 different solvents. The correlation between the reaction driving force ($-\Delta G_r$) and activation barrier (ΔG^\ddagger) has been explored in order to understand the solvent effects (static and dynamic) on the photo-excited ICT reaction in this molecule. A Kramer's model analysis of the experimentally observed reaction rate constants indicates a solvent-averaged activation barrier of $\sim 4 k_B T$ in the absence of solvent dynamical control. The reaction in M6C is therefore not a barrier-less reaction but close to the limit where conventional kinetics might break down.

Keywords. ICT reaction; solvent effects; hetero atom replacement.

1. Introduction

Excited state intramolecular charge transfer (ICT) reactions in substituted aminobenzonitrile derivatives have been an area of intense research for quite some time now.^{1–5} While potential applications of ICT molecules in designing fluorescent dyes,^{6–7} electron transfer photochemistry,⁸ solar collectors,⁷ pH or ion indicators^{9,10} have driven much of the interest in industry, quest for fully understand the basic scientific aspects of ICT reactions in various media continues to attract attention of physical chemists. Photo-induced charge transfer is an important process in biology as light-induced charge separation plays key roles in photosynthesis and vision. Since a small barrier of a few $k_B T$ is sometimes associated with the ICT reaction in many molecules, interpretation of static and dynamic solvent control of reaction in these molecules becomes more complex. A two-state model is sometimes used to describe the excited state ICT reaction which, in the absence of solvation dynamics within the observation time, predicts a bi-exponential kinetics.^{5,11–13} A deviation from the bi-exponential kinetics then signals the break-down of the conventional high-barrier kinetics.

The molecule that we are considering in this work is 4-(morpholenyl)benzonitrile (M6C) which contains an oxygen atom in a position *para* to the nitrogen atom of the donor moiety (see scheme 1). Typical to



Scheme 1.

*For correspondence

many DMABN derivatives, this molecule also show two fluorescence emission bands in polar solvents and only one band in non-polar solvents. The appearance of two emission bands in polar solvents is a reflection of intramolecular charge transfer reaction in the excited state and several models have been proposed to explain the new emission in polar environments.¹ The new emission in polar molecules are believed to occur from an electronic state of charge transfer (CT) character, whereas the normal fluorescence is from a locally excited (LE) character with charge distribution similar to that in the ground state. Upon photoexcitation, a substantial amount of charge is transferred from the amino group to benzonitrile moiety forming the CT state. Consequently, the more polar CT state is further stabilized by polar solvent via enhanced dipole–dipole interaction between dipolar solvent molecules and photoexcited solute.

We will use the twisted intramolecular charge transfer (TICT) model to explain the photo-induced charge transfer reaction in the M6C. Eventhough other models are also used to explain the CT emission in hindered DMABN derivatives, TICT model has been found to be suitable for unhindered molecules like the one which is being considered in this work. According to the twisted intramolecular charge transfer (TICT) model, the charge transfer process occurs with the simultaneous twisting of the bond connecting the amino group and the benzene ring.^{1–5} Further evidence for the TICT mechanism comes from the experimentally observed solvent dynamical control of the LE \rightarrow CT conversion reaction rate.^{12–15} The agreement between theory and experiments found in our earlier studies in electrolyte solutions^{12,13} also provides support to the TICT mechanism for the excited state intramolecular charge transfer reaction. As shown in scheme 1, photo-excitation promotes M6C to the locally excited (LE) state in the first excited electronic surface (S_1). The photo prepared LE state then either undergoes intramolecular charge transfer with the forward reaction rate constant k_f or comes back to the ground state (S_0) with an average (radiative + nonradiative) rate constant (k_{LE}). Likewise, the charge transferred (CT) state can go back to the LE state with a rate constant of k_r or populate the ground state via the average (radiative and non-radiative) rate constant k_{CT} . As already discussed,⁵ such a two state model with time-independent rate constants is expected to generate bi-exponential emission decays for M6C in polar solvents, provided solvent dynamics is not

seen during the time scale of the interconversion reaction.

The main results of the paper are as follows. Quantum yield, radiative and non-radiative rates, transition moments and changes in reaction free energy (reaction driving force) for M6C have been determined in ~ 20 different solvents and compared with a closely related molecule, 4-(1-piperidinyl)-benzonitrile P6C. These solvents provide a good spread of solvent field factor as the static dielectric constant (ϵ_0) ranges from ~ 2 to 110. Bi-exponential decay kinetics has been found for M6C in all the polar solvents studied and therefore the LE \rightarrow CT interconversion reaction in this molecule conforms to the two-state reversible reaction mechanism.⁵ Correlations between the solvent polarity and changes in reaction free energy, and reaction rate constant are attempted to explore the solvent effects on the ICT reaction in this molecule. Average activation energy has been estimated by using Kramer's type model for the barrier crossing and a barrier of $\sim 4 k_B T$ is found in the absence of dynamic solvent effects on the ICT reaction. Note that the ICT molecule under study (M6C) has been used in of our earlier study^{16(a)} to characterize the encapsulated polar solvent pools inside reverse micelles. In that study, the average rate-constant of TICT reaction in this molecule has been used as a probe to acquire information about the static and dynamic medium effects on chemical reaction^{16(b)} in confined aqueous environments. A comparatively larger solubility of M6C in water has been particularly helpful in that study.^{16(a)} However, the photophysics and photodynamics of M6C have not been studied before and the present work provides a thorough study of these aspects of this ICT molecule in bulk solvents at ambient condition.

The organization of the rest of the article is as follows. Experimental details are discussed in the next section. Section 3 contains the experimental results, analysis of which are based on equations derived in ref. 5 and discussion on photophysics and photodynamics of M6C molecule in various solvents. Finally, the concluding remarks are given in section 4.

2. Experimental

4-(1-morpholenyl) benzonitrile (M6C) was synthesized by following the protocol given in the literature.¹⁷ Steady state absorption spectra were recorded by using a spectrophotometer (Shimadzu, UV-2450).

Steady state emission spectra were recorded by using a fluorimeter (SPEX fluoromax-3, Jobin-Yvon, Horiba) after adjusting the absorbance of the sample to ~ 0.1 . Measurements were made by taking the solutions in an optically transparent, quartz cuvette with 1 cm optical path length. For a given sample, the peak wavelength (λ) of the absorption spectrum was used as excitation wavelength for the corresponding emission scan. The fluorescence spectra were properly corrected before extracting relevant quantities from them. Samples bubbled with dry nitrogen gas show no effects on the overall appearance of the spectra for M6C in solutions and also on its decay kinetics.

Average peak frequencies of the absorption and emission spectra were obtained from various measures of the frequencies as before. The area under the LE and CT emission bands were determined by shifting and broadening a reference emission spectrum of M6C in a non-polar solvent, keeping constant the total area under the emission spectrum in a given polar solvent. The error associated with the peak frequency determination is typically $\pm 250 \text{ cm}^{-1}$ and that with the band area is $\sim 10\%$ (of the reported value), unless otherwise mentioned.

Time-resolved fluorescence emission intensity decay for M6C in these solvents were collected by using a time-correlated single photon counting (TCSPC) instrument based on a picosecond Ti: sapphire laser with excitation light wavelength at 300 nm (third harmonic). The emission fluorescence was collected at magic angle at both LE and CT peak positions (of steady-state spectrum) with an emission band-pass of 8 nm. The effective resolution (full width at half maximum, fwhm) of the instrument response function (IRF) was $\sim 100 \text{ ps}$. Subsequently, decays were deconvoluted from IRF and fitted to multiexponential function using an iterative reconvolution algorithm.⁵ Such fitting enables one to capture decay kinetics with time constant as fast as $\sim 20 \text{ ps}$ with reasonable accuracy. For a few samples, emission decays collected at a few wavelengths near the LE or CT peak positions were analysed and the analysed data were found to vary within a small uncertainty. Note that emission intensity decays for M6C in non-polar solvents were found to be single-exponential collected at any wavelength across its steady state emission band. These decays fit with one large time constant which is different from the small time constant obtained from the bi-exponential decay in polar solvents. All the measurements reported here were performed at $T(\text{K}) = 298 \pm 0.1$.

3. Results and discussion

Figure 1 displays absorption and emission spectra of M6C in heptane ($\epsilon_0 \sim 2$), ethyl acetate ($\epsilon_0 \sim 6$) and acetonitrile ($\epsilon_0 \sim 36$). As expected, both the absorption and emission spectra show red-shift as the solvent becomes more polar. In addition, both the LE and CT emission bands appear as the non-polar heptane is replaced by a moderately polar solvent, ethyl acetate. When the solvent's polarity becomes as large as that of acetonitrile, CT emission absolutely dominates the spectrum. Similar polarity-induced domination of CT population has been observed earlier⁵ with a closely related molecule, P6C. However, both absorption and emission spectra in a given solvent of these two molecules (M6C and P6C) differ appreciably, even though both these molecules possess very similar six-membered rings as donor groups. A representative of this sort is presented in

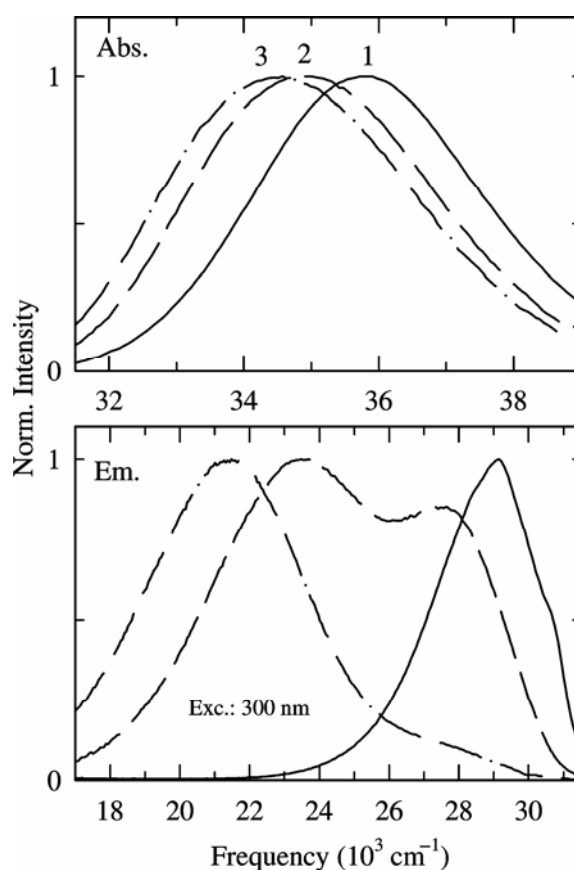


Figure 1. Absorption and emission spectra of 4-(1-morpholenyl) benzonitrile (M6C) in solvents of differing polarities: heptane (solid line, 1), ethyl acetate (long dash, 2), acetonitrile (dash-dot, 3). Upper panel represents the absorption spectra and lower panel the emission spectra.

figure 2 where absorption and emission spectra of these two molecules in ethyl acetate are shown. It is evident from this figure that both the absorption and CT emission bands of M6C is $\sim 700\text{ cm}^{-1}$ blue-shifted than those for P6C in ethyl acetate. This indicates that both the ground and excited states of M6C are less polar than in P6C, signalling relatively more contribution of the less polar L_b state in the transition moments of M6C.⁵

Characteristics of the absorption and emission spectra of M6C were determined in 20 different solvents that provide a good spread of the dielectric reaction field factor,

$$d_c(\epsilon_0) = \frac{\epsilon_0 - 1}{2(1-c)\epsilon_0 + (1+2c)},$$

where c , ranging between 0 and 1, effectively accounts for solute polarizability effects. We have used $c = 0.25$ since this produces the best correlation.⁵

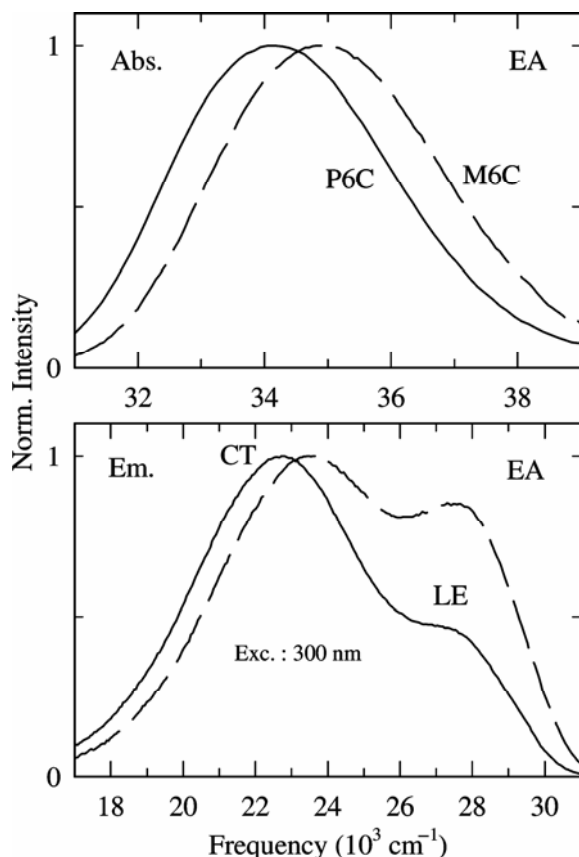


Figure 2. A comparison between the absorption (upper panel) and emission (lower panel) spectra of 4-(1-morpholenyl) benzonitrile (M6C) and 4-(1-piperidinyl) benzonitrile (P6C) in ethyl acetate. Note the relative blue shift in the spectra of M6C.

Table 1 lists these solvents and summarizes the steady state spectral data. Since one of our goals is to understand the solvent effects (both static and dynamic) on the ICT reaction in M6C, we explored correlations of various spectral quantities with the reaction field factor described above. One of such correlations is presented in figure 3. The first two panels of this figure are essentially the depiction of what has already been observed in figure 1 for a few solvents. Data in protic polar solvents are shown by separate symbols (triangles) in order to find out if the solute-solvent specific (H-bonding) interaction plays any role. It is interesting to note that the area ratio, α_{CT}/α_{LE} in methanol is ~ 2.5 times larger than

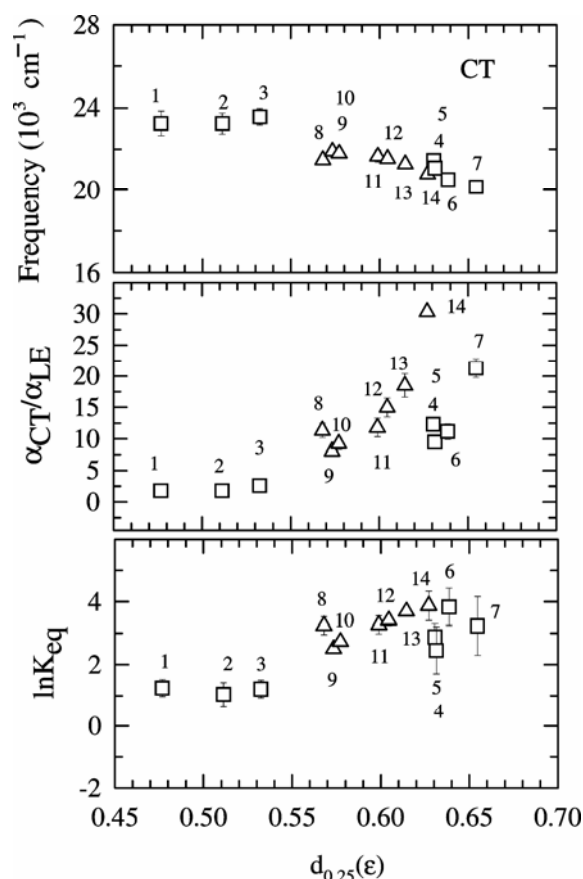


Figure 3. Correlations of peak frequency associated with CT band, the ratio (α_{CT}/α_{LE}) between areas under the CT and LE bands, logarithm of equilibrium constant (K_{eq}) with solvent dielectric factor, $d_{0.25}(\epsilon_0)$. Data for protic polar solvents are represented by triangles and those for aprotic solvents by squares. Solvents are marked with numbers, which are assigned as follows: 1 (EA), 2 (THF), 3 (DCM), 4 (acetonitrile), 5 (DMF), 6 (DMSO), 7 (formamide), 8 (TBA), 9 (hexanol), 10 (pentanol), 11 (2-methyl-1-propanol), 12 (propanol), 13 (ethanol), 14 (methanol). Large error bars associated measurements in those solvents where one of the bands had less than 10% of the total area under the whole emission band.

Table 1. Steady state spectral properties of M6C in different solvents.

Solvent	ϵ_0	n_D	ν_{abs}	ν_{LE}	ν_{CT}	Γ_{abs}	Γ_{LE}	Γ_{CT}	α_{CT}/α_{LE}	K_{eq}	$-\Delta G_r$
PFH	1.76	1.252	36.56	29.04	–	3.70	3.61	–	–	–	–
Heptane	1.92	1.388	35.85	28.83	–	3.98	3.67	–	–	–	–
Hexane	2.00	1.375	35.92	–	–	3.97	–	–	–	–	–
Cyclohexane	2.02	1.424	35.74	28.66	–	3.96	3.63	–	–	–	–
Diethyl ether	4.20	1.350	35.41	27.66	–	4.16	3.97	–	–	0.13	–5.14
Ethyl acetate	6.02	1.370	35.04	27.78	23.24	4.30	1.18	5.80	1.78	3.48	3.09
THF	7.58	1.405	34.66	27.78	23.24	4.02	1.18	5.80	1.78	2.83	2.57
DCM	8.93	1.421	34.66	27.79	23.58	4.31	0.94	3.83	2.62	3.36	3.00
TBA	12.5	1.387	34.88	27.38	21.48	4.55	2.09	4.32	11.32	25.51	8.03
Hexanol	13.3	1.415	34.79	27.61	21.90	4.54	1.60	4.35	8.05	12.19	6.2
Pentanol	13.9	1.407	34.77	27.55	21.80	4.55	1.75	4.31	9.24	15.31	6.76
IBA	18.7	1.396	34.77	27.39	21.66	4.54	1.84	4.27	11.80	26.15	8.09
Propanol	20.45	1.384	34.76	27.56	21.55	4.54	1.66	4.39	14.97	30.32	8.46
Ethanol	24.55	1.359	34.80	27.45	21.28	4.56	1.69	4.37	18.49	40.25	9.16
Methanol	32.66	1.327	34.78	27.31	20.79	4.6	1.73	4.39	30.35	48.21	9.61
Acetonitrile	35.94	1.342	34.71	27.04	21.46	4.36	1.96	3.92	12.30	17.76	7.13
DMF	36.71	1.428	34.49	26.45	21.08	–	2.82	3.67	9.48	11.62	6.08
DMSO	46.45	1.478	34.09	25.85	20.53	4.38	3.36	3.61	11.15	46.34	9.51
Formamide	111.00	1.447	34.18	25.47	20.16	4.57	2.5	3.93	21.27	25.22	8.00

Avg. frequency (ν) and full width at half maxima (Γ) are expressed in 10^3 cm^{-1} . $-\Delta G_r$ are in kJ mol^{-1} units. PFH: perfluorohexane, DCM: Dichloromethane, THF: Tetrahydrofuran, TBA: Tertiary butyl alcohol, IBA: Isobutyl alcohol, DMF: Dimethyl formamide, DMSO: Dimethyl sulfoxide.

that in acetonitrile even though the latter is somewhat more polar than the former. Earlier studies with P6C also reported similar relative enhancement in methanol.⁵ Whether these results indicate H-bonding interaction between M6C and polar protic solvents is not certain but it is clear in this figure that area ratio is uniformly larger in polar protic solvents than that in the polar aprotic ones. The inverse correlation between the CT frequency and the area ratio, α_{CT}/α_{LE} , for M6C in pure solvents suggest that the dielectric field factor is responsible for both the red shift in the CT emission spectrum and enhancement of its population.

Since the area ratio is increasing linearly with the solvent dielectric field factor, the equilibrium constant for the LE \rightarrow CT conversion reaction in M6C is also expected to increase in the similar manner. The last panel of figure 3 shows the expected behaviour. Note that the equilibrium constant shown in this panel is a *mean* of the equilibrium constants determined from the steady state and time resolved studies. The steady state equilibrium constant is obtained from the area ratio,⁵

$$K_{eq}^{\alpha} \approx \frac{\alpha_{CT} \nu_{LE}^3}{\alpha_{LE} \nu_{CT}^3}$$

where the frequency factor takes care of the difference in radiative rates between the LE and CT

states. Equilibrium constant can be estimated from time resolved studies by simply taking the ratio between the decay components, $K_{eq}^a = a_{rxn}/a_{dec}$. Note a_{rxn} is the amplitude of the component associated with the short (reaction) time constant and a_{dec} with the long (population decay) time constant. It is clear from this panel that the average equilibrium constant (K_{eq}) increases by a factor of ~ 50 on changing the solvent from diethyl ether ($\epsilon_0 \sim 4$) to acetonitrile ($\epsilon_0 \sim 36$). The strong correlations depicted in these three panels therefore suggest that the ICT reaction in M6C involves a sizeable barrier and the solvent polarity modifies it significantly. However, these correlations cannot indicate the extent of solvent dynamical control of the same reaction in these solvents. Correlation between the reaction rate and changes in reaction free energy ($-\Delta G_r$) found in earlier studies⁵ have indicated a rather limited role of solvent dynamical modes in modifying the reaction rate in these unhindered DMABN derivatives.

Before we present experimental results on the solvent dependence of the reaction rate constant and its correlation with solvent dielectric properties, let us investigate the solvent dependence of other solute properties, such as, quantum yield, radiative and non-radiative rates, and transition moments (absorption and emission). We have measured these quantities for M6C in many of these solvents and the data are summarized in table 2. The relations

Table 2. Quantum yield, radiative, non-radiative rates of M6C in different solvents.

Solvent	Φ_{net}	Φ_{LE}	Φ_{CT}	$k_{\text{LE}}^{\text{rad}} (10^7 \text{ s}^{-1})$	$k_{\text{LE}}^{\text{nr}} (10^9 \text{ s}^{-1})$
PFH	0.033	0.033	–	2.53	0.74
Heptane	0.068	0.068	–	3.32	0.46
Hexane	0.064	0.064	–	3.19	0.47
Cyclohexane	0.138	0.138	–	6.23	0.39
Diethyl ether	0.080	0.080	–	4.26	0.49
Ethyl acetate	0.039	0.014	0.025	2.31	1.63
THF	0.047	0.017	0.030	1.97	1.14
DCM	0.086	0.024	0.062	2.64	1.07
TBA	0.035	0.003	0.032	2.13	7.08
Hexanol	0.041	0.005	0.036	1.08	2.15
Pentanol	0.041	0.004	0.037	1.12	2.79
IBA	0.037	0.003	0.034	2.47	8.19
Propanol	0.038	0.002	0.036	1.47	7.34
Ethanol	0.032	0.002	0.030	2.34	11.66
Methanol	0.022	0.001	0.021	0.96	9.6
Acetonitrile	0.028	0.002	0.026	0.66	3.28
DMF	0.04	0.004	0.036	0.43	1.07
DMSO	0.03	0.002	0.028	4.04	20.16
Formamide	0.018	0.001	0.017	0.11	1.12
NMF	0.015	–	0.015	–	–

Quantum yields (Φ) for M6C in different solvents are tabulated. Φ_{LE} and Φ_{CT} are the quantum yields for individual parts. $k_{\text{LE}}^{\text{rad}}$ and $k_{\text{LE}}^{\text{nr}}$ denote respectively the radiative and non-radiative rates associated with the LE band. Estimated errors for these calculations are within $\pm 10\%$ about the average for most of the cases

that are used to calculate these quantities from steady state and time resolved data are already described in many places⁵ and therefore we discuss only the results here. The values of the net quantum yield (ϕ_{net}), and those of the individual components, ϕ_{LE} and ϕ_{CT} , for M6C in these solvents are comparable to those for P6C. As expected, the radiative rates are smaller and non-radiative rates larger in protic solvents than those in aprotic solvents. As found earlier⁵ for closely related molecules, both absorption and LE transition moments are found to be solvent insensitive and their values are $\sim 4 \text{ D}$ and $\sim 1 \text{ D}$, respectively.

The reaction time constants (or simply the reaction times) are obtained by fitting either the LE or CT emission intensity decays of M6C in various polar solvents. As already stated, the emission intensity decay of M6C in most of the polar solvents was found to adequately fit with bi-exponential function of time. One such fitting is shown in figure 4 along with residuals in the bottom panel for M6C in tetrahydrofuran. Parameters obtained from fits for various solvents are summarized in table 3. The representative fitting shown in figure 4 together with the ‘goodness-of-fit’ parameter (χ^2) in table 3 suggest that the emission decays of M6C in these polar solvents are indeed bi-exponential functions of time.

In order to ensure that the fast time constant in the LE decay is indeed associated with the LE \rightarrow CT conversion reaction of M6C, we have also analysed the CT emission decays and compared the fast time constants (‘rise-time’) with those from the LE decays. Representative fits to the intensity emission decays of M6C in ethyl acetate are shown in figure 5. Fit parameters shown in the inset suggest that the CT rise time is quite close to that associated with the fast component of the LE decay. This means that the fast time constant found in the LE decay is essentially the LE \rightarrow CT conversion reaction in M6C in this solvent. Similar level of agreement has been observed in most of the cases (IRF permitting) and thus the fast time constant is regarded as the ICT reaction time constant in M6C.

We next explore the correlations of $-\Delta G_r$ and the forward reaction rate constant (k_f) obtained for M6C in various polar solvents with solvent dielectric field factor and compare them with those of P6C. The following formula has been used to calculate k_f from the reaction time (τ_{rxn}) and equilibrium constant,

$$k_f = \frac{1}{\tau_{\text{rxn}}(1 + K_{\text{eq}}^{-1})}$$

Table 3. Decay of M6C associated with LE band: fit parameters.

Solvent	a_1	a_2	τ_1 (ns)	τ_2 (ps) ^b	χ^2	a_{rxn}/a_{dec}
PFH	1		1.30		1.25	
Heptane	1		2.05		1.34	
Hexane	1		2.01		1.30	
Cyclohexane	1		2.22		1.42	
Diethyl ether	0.80	0.20	2.32	119	1.15	0.25
Ethyl acetate	0.20	0.80	2.92	<20 (17)	1.14	3.93
THF	0.28	0.72	3.06	23	1.10	2.61
DCM	0.29	0.71	3.07	<20 (18)	1.28	2.42
TBA	0.04	0.96	3.22	29	1.17	27.57
Hexanol	0.11	0.89	3.19	133	1.83	8.26
Pentanol	0.08	0.92	3.50	94	1.97	11.99
IBA	0.03	0.97	2.73	30	1.15	28.41
Propanol	0.03	0.97	3.27	29	1.56	29.30
Ethanol	0.02	0.98	2.96	<20 (15)	1.11	40.67
Methanol	0.04	0.96	2.56	<20 (15)	1.47	27.57
Acetonitrile	0.09	0.91	3.43	<20 (14)	1.09	10.76
DMF ^a	0.51	0.49	3.53	34	1.60	0.96
DMSO	0.01	0.99	3.18	<20 (5)	1.36	70.43

^aLE emission could not be collected because of its negligible population in this solvent. Note that short time constants of the bi-exponential fit of LE population decays, τ_2 (ps) in the above table, are the reaction times in the corresponding solvents.

^bNumbers in parenthesis in this column denote the values of reaction time constant obtained from fits to the collected emission intensity decays. Since these numbers are smaller than the one-fifth of the instrument response function (~ 100 ps), it is better to consider them as reaction time-scales faster than 20 ps.

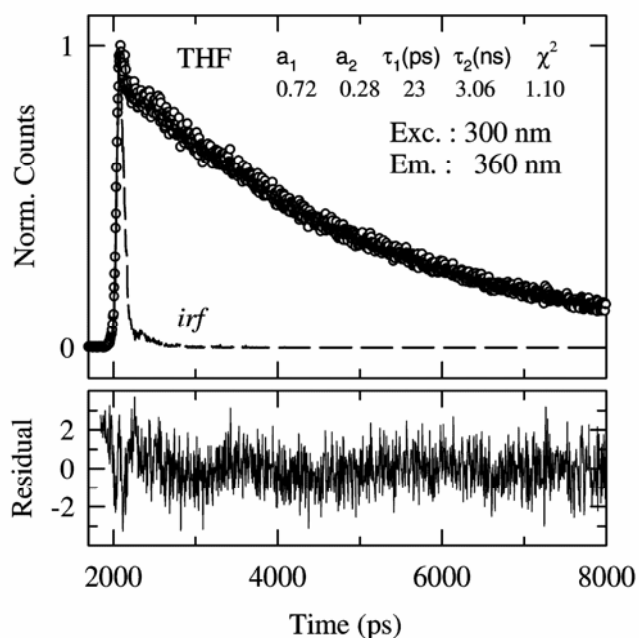


Figure 4. Representative LE emission decay of M6C in tetrahydrofuran (THF, $\epsilon_0 \approx 7.6$) and its bi-exponential fit. The data are represented by the circles, while the fit through the data are by the solid line. The instrument response function is shown by the broken line. The fit (bi-exponential) results are also provided in the inset. The LE peak count is ~ 2000 . Residuals are shown in the bottom.

The calculated values of $-\Delta G_r (= RT \ln K_{eq})$ and k_f are shown as a function of $d_c(\epsilon_0)$ with $c = 0.25$ in figure 6. The relevant results for P6C are also shown⁵ (filled circles) in the same figure. A comparison between these two sets of data indicates that the solvent polarity dependence of the reaction driving force ($-\Delta G_r$) and the reaction rate constant are very similar for these two reactants. This means that the presence of the oxygen atom in the donor moiety does not affect the reaction except decreasing the ground and excited state dipole moments of the reactant.

We next estimate the reaction barrier (ΔG^\ddagger) that the LE \rightarrow CT conversion reaction in M6C experiences in different polar solvents. In a Kramer's type model, the barrier crossing¹⁸⁻²⁰ rate can be expressed

$$k_f = \kappa \nu_R \exp(-\Delta G^\ddagger / k_B T), \quad (1)$$

where ν_R denotes the reactant well frequency and κ the frictional transmission co-efficient ($\kappa \leq 1$). Solvent dependent ΔG^\ddagger can then be easily estimated from the experimentally obtained k_f if we assume that the reactant well frequency for M6C is the same as that found for P6C ($\nu_R \sim 2 \times 10^{12} \text{ s}^{-1}$) and the solvent dynamic effects on the reaction are completely

absent ($\kappa = 1$). The *average* of the barrier heights so obtained is found to be approximately $4 k_B T$ which is again very close to what has been estimated earlier for P6C in the same solvent friction limit.⁵

Next we explore how the forward reaction rate constant and the activation energy are correlated to the reaction driving force, ΔG_r . Data in figure 7 reveal that a strong correlation between k_f and ΔG_r exists (upper panel). Interestingly, the correlation curves indicate different slopes for polar protic and aprotic solvents. Note that similar difference between these two types of solvents has also been observed for the solvent dependence of area ratio and equilibrium constant (see figure 3). Despite the difference in slopes, the strong correlation suggests

that the reaction rate constant is significantly influenced by ΔG_r in both types of solvents and this influence arises mainly from the modulation of the barrier height (ΔG^\ddagger). As shown in the lower panel of figure 7, ΔG^\ddagger is linearly related to ΔG_r for M6C in these solvents and asserts the relation,⁵ $\Delta G^\ddagger \approx \alpha \Delta G_r$. Separate linear fits of the data shown in this panel to the above relation produce 0.6 and 0.18 for α in protic and aprotic polar solvents, respectively. The average of these two values is ~ 0.4 which is again very close to what has been found earlier for P6C.

An interesting consequence of the different slopes of ΔG^\ddagger versus ΔG_r curves for protic and aprotic polar solvents would be that the reaction in methanol should proceed with a faster rate constant than that in acetonitrile. However, the present experimental data do not show such a difference (see table 3).

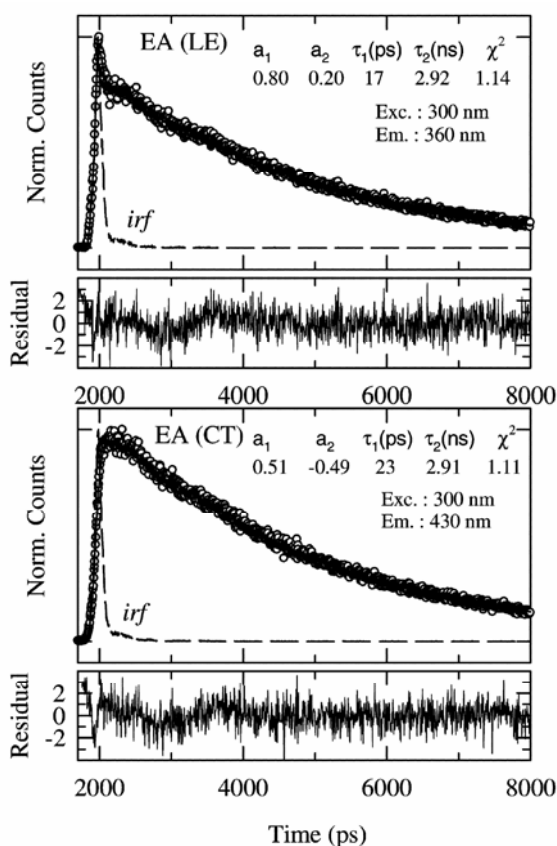


Figure 5. LE emission decay (upper panel) and CT emission decay (lower panel) of M6C in ethyl acetate (EA, $\epsilon_0 \approx 6$) and its bi-exponential fit. The line represents a bi-exponential fit through the experimental data (circles). Fit parameters are shown in the inset. Residuals are shown at the bottom of each panel. Fit parameters shown in the inset suggest that the CT rise time is quite close to that associated with the fast component of the LE decay in the upper panel. This means that the fast time constant found in the LE decay is essentially the LE \rightarrow CT conversion reaction in M6C in this solvent.

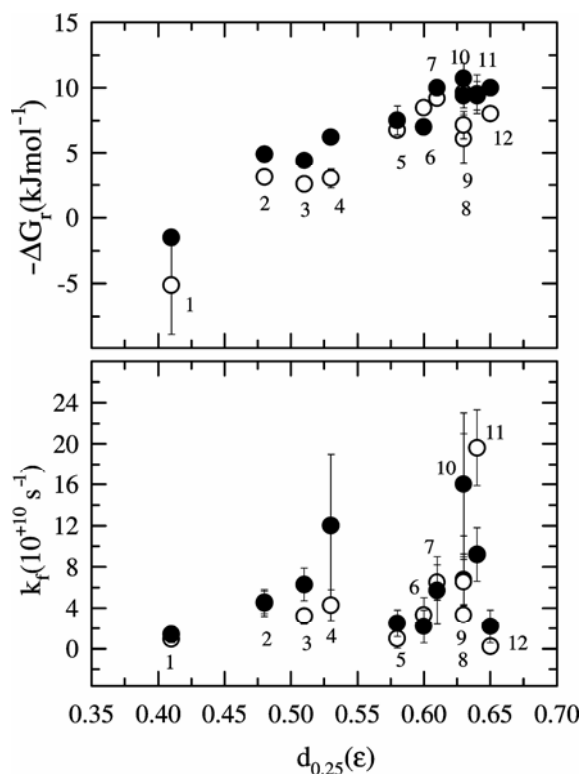


Figure 6. Comparison between M6C and P6C. Gibbs free energy change ($-\Delta G_r$) and forward reaction rate constant (k_f) are shown as a function of solvent dielectric field factor. Open and filled symbols represent the data respectively for M6C and P6C. Solvents are marked with numbers, which are assigned as follows: 1 (DEE), 2 (EA), 3 (THF), 4 (DCM), 5 (pentanol), 6 (propanol), 7 (ethanol), 8 (DMF), 9 (acetonitrile), 10 (methanol), 11 (DMSO), 12 (formamide). Note large error bars in P6C data (from ref. 5) for some solvents in which LE area was found to be very small.

This is because the reaction time constants of M6C in these two ‘ultrafast’ solvents are much shorter than the effective time resolution of the instrument (~ 100 ps). The similarity in reaction time constants for P6C in methanol and acetonitrile (7 ps and 8 ps) was also found earlier with a much better time resolution (~ 25 ps).⁵ Therefore, the present results for M6C in these two solvents (~ 15 ps) are in corroboration with what has already been observed earlier with P6C.

The reliability of the measured average reaction times of less than 100 ps which the present study reports (see table 3) for M6C in a number of solvents considered here warrants further discussion. Since measured reaction time in many of the solvents considered here is much faster than the time resolution, any inaccuracy in measurements can give rise to

incorrect values of thermodynamic and kinetic parameters calculated using these reaction times, leading to erroneous conclusions. Fortunately, it has been shown elsewhere that a dynamical event with time constant of as fast as one-fifth of the IRF can be measured with some confidence if iterative reconvolution method is employed to extract fit-parameters from the collected intensity decays.⁵ In one of our earlier studies on solute rotation in alcohol solvents,²¹ a comparative study has shown that we could reliably measure a time constant of ~ 15 ps employing a time resolution of ~ 75 ps (see table 3 of ref. 21). We expect that this accuracy is also extended to the present measurements and thus reaction times $\sim 20 \geq \tau_{\text{rxn}}(\text{ps}) \leq 50$ are semi-quantitatively correct. In addition, our earlier works with TICT reaction of closely related molecules in various media^{11,13,16(b),22} have reported time constants < 100 ps measured with time resolution as broad as ~ 475 ps. Even though such data may question the reliability of the measurements, our measured time constants with IRF ~ 475 ps seemed to have compared well with some previously measured reaction time constants⁵ with time resolution as sharp as ~ 25 ps. These favourable comparisons have led us to believe that the reaction time constants reported here for M6C in bulk polar solvents are indeed meaningful and can generate a semi-quantitative description of solvent dependence of the TICT reaction in M6C. However, we caution that a time constant of ~ 5 ps (for DMSO) may not represent the real time scale and thus should be considered with lesser degree of confidence.²³ In spite of the above discussion, conclusions drawn from this work remain *unaltered* as the calculation of *average* equilibrium constant (K_{eq}) involves only the amplitudes of the decay components, *not* the reaction time constants.

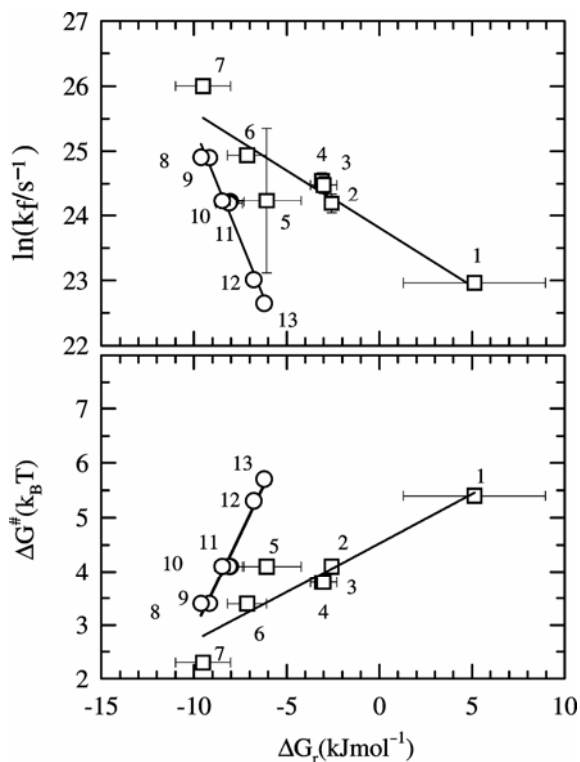


Figure 7. Upper panel: Logarithmic forward rate constant ($\ln k_f$) versus the reaction driving force (ΔG_r) of the LE \rightarrow CT reaction. Open and filled symbols represent respectively polar protic and aprotic solvents. Solid lines represent linear fits through the data. Solvents are marked with numbers, which are assigned as follows: 1 (DEE), 2 (THF), 3 (DCM), 4 (EA), 5 (DMF), 6 (acetonitrile), 7 (DMSO), 8 (methanol), 9 (ethanol), 10 (propanol), 11 (2-methyl-1-propanol), 12 (pentanol), 13 (hexanol). Lower panel: Relationship between the barrier heights ΔG^\ddagger and reaction driving force (ΔG_r). Representations remain the same as in the upper panel.

4. Conclusion

To summarize, the replacement of the carbon atom *para* to the nitrogen atom of the six-membered donor moiety of P6C does not lead to any appreciable change in reaction driving force or activation barrier. Reaction driving force and activation free energy are found to be linearly correlated with an average slope of ~ 0.4 . The correlation between the reaction rate constant and the estimated activation barrier in the limit of zero solvent friction produces an activation barrier of $\sim 4 k_B T$ for this ICT molecule. All these results are similar to those obtained

for P6C. The only effect of the oxygen replacement in the donor moiety has been the blue shift of the absorption and emission spectra of M6C in a given solvent relative to those of P6C.

Temperature-dependent studies of the reaction rate in these solvents should be carried out to estimate the 'actual' barrier height involved in the ICT reaction of M6C in these solvents. One may also like to carry out quantum chemical calculations in order to find out why insertion of the oxygen atom induces blue shift in spectra relative to those in P6C. If the difference in slopes between protic and aprotic solvents are any indication of different solute-solvent interactions for M6C, then this molecule's better solubility can be used to study electrolyte effects in water-rich environments. The fast reaction time constant of M6C can also be used to probe the spatial and temporal scales of heterogeneity in molten non-aqueous electrolyte mixtures where the system is expected to behave as super-cooled solutions.²⁴ Some of the above works are already in progress and we hope to report them soon.

Acknowledgements

Financial supports from the Council of Scientific and Industrial Research (CSIR), India is gratefully acknowledged. TP acknowledges the University Grants Commission (UGC), India and HG thanks SN Bose National Centre for Basic Sciences (SNBNCBS) for research fellowships. In addition, HG expresses his sincere thanks to the Vice Chancellor, Aliah University, West Bengal for encouragement.

References

1. Grabowski Z R, Rotkiewicz K and Rettig W 2003 *Chem. Rev.* **103** 3899
2. Lippert E, Rettig W, Bonacic-Koutecky V, Heisel F and Mieche J A 1987 *Adv. Chem. Phys.* **68** 1
3. Zachariasse K A, Druzhinin S I, Bosch W and Machinek R 2004 *J. Am. Chem. Soc.* **126** 1705
4. Techert S and Zachariasse K A 2004 *J. Am. Chem. Soc.* **126** 5593
5. Dahl K, Biswas R, Ito N and Maroncelli M 2005 *J. Phys. Chem.* **B109** 1563
6. Rettig W 1986 *Angew. Chem. Int. Ed.* **250** 971
7. Rettig W 1991 *Nachr. Chem. Tech. Lab.* **39** 298
8. Habib Jiwan J L and Soumillion J P 1992 *J. Photochem. Photobiol.* **A64** 145
9. Rettig W and Wolfbesis O S 1993 *Fluorescence spectroscopy new methods and applications* (Springer Berlin) p. 31
10. Plaza P, Jung N D, Martin M M, Meyer Y H, Vogel M and Rettig W 1992 *Chem. Phys.* **1680** 365
11. Pradhan T, Ghoshal P and Biswas R 2008 *J. Phys. Chem.* **A112** 915
12. Pradhan T and Biswas R 2007 *J. Phys. Chem.* **A111** 11514
13. Pradhan T and Biswas R 2007 *J. Phys. Chem.* **A111** 11524
14. Pradhan T, Ghoshal P and Biswas R 2009 *J. Chem. Sci.* **121** 95
15. Braun D and Rettig W 1997 *Chem. Phys. Lett.* **268** 110
16. (a) Biswas R, Rohman N, Pradhan T and Buchner R 2008 *J. Phys. Chem.* **B112** 9379; (b) Pradhan T, Gazi H A R and Biswas R 2009 *J. Chem. Phys.* **131** 054507
17. (a) Rettig W 1980 *J. Luminesc.* **26** 21; (b) Rettig W 1982 *J. Phys. Chem.* **86** 1970
18. Zwan vander G and Hynes J T 1991 *Chem. Phys.* **152** 169
19. Hynes J T 1985 *The theory of reactions in solution in the theory of chemical reactions* (ed.) M Baer and I G Crizmadia (Boca Raton: CRC Press) p. 171
20. Fleming G R and Hanggi P 1993 *Activated barrier crossing* (Singapore: World Scientific)
21. Pradhan T, Ghoshal P and Biswas R 2008 *J. Chem. Sci.* **120** 275
22. Pradhan T and Biswas R 2009 *J. Soln. Chem.* **38** 517
23. Bevington P R 1969 *Data reduction and error analyses for the physical sciences* (New York: MacGraw-Hill)
24. Guchhait B, Gazi H A R, Kashyap H K and Biswas R 2010 *J. Phys. Chem.* **B114** 5066